Optics Letters

Estimation of C_n^2 based on scintillation of fixed targets imaged through atmospheric turbulence

Damián Gulich,[1,2,3,*] Gustavo Funes,[4] Darío Pérez,[5] and Luciano Zunino[1,2]

[1]Centro de Investigaciones Ópticas (CONICET La Plata-CIC), C.C. 3, 1897 Gonnet, Argentina
[2]Departamento de Ciencias Básicas, Facultad de Ingeniería, Universidad Nacional de La Plata (UNLP), 1900 La Plata, Argentina
[3]Departamento de Física, Facultad de Ciencias Exactas, Universidad Nacional de La Plata (UNLP), 1900 La Plata, Argentina
[4]Facultad de Ingeniería y Ciencias Aplicadas, Universidad de los Andes Mons. Alvaro del Portillo 12455, Las Condes, 7620001 Santiago, Chile
[5]Instituto de Física, Facultad de Ciencias, Pontificia Universidad Católica de Valparaíso (PUCV), Av. Brasil 2950, 234-0025 Valparaíso, Chile
*Corresponding author: dgulich@ciop.unlp.edu.ar

Received 29 September 2015; revised 31 October 2015; accepted 3 November 2015; posted 3 November 2015 (Doc. ID 250918); published 26 November 2015

We define a pixel-based scintillation index for dynamic incoherent imaging of fixed high-contrast targets through atmospheric turbulence. We propose a simple setup to study this parameter varying the C_n^2 constant in controlled laboratory conditions (weak fluctuation regime). We find the semi-empirical relationship between the pixel-based scintillation index and the index of refraction structure constant, which we then employ to estimate C_n^2 successfully in an independent case in which this value was not known beforehand.

OCIS codes: (010.1300) Atmospheric propagation; (010.1330) Atmospheric turbulence; (010.7060) Turbulence; (030.4280) Noise in imaging systems; (100.2000) Digital image processing; (110.0115) Imaging through turbulent media.

http://dx.doi.org/10.1364/OL.40.005642

Around 1610, Galileo briefly reported the effect of atmospheric turbulence on astronomical imaging [1]. This phenomenon occurs because atmospheric turbulence produces a dynamic blur, degrading the records of fixed targets. Turbulence parameters can be extracted from imaging [2,3], while the knowledge of these parameters allows us to simulate its effects [4]. The estimation of atmospheric turbulence parameters and the simultaneous correction of blurring in dynamic imaging of a high-contrast target have recently been studied by Gibson and Hammel [5]. In this Letter, we propose a simple technique to estimate C_n^2 based on pixel intensity fluctuations by imaging a fixed high-contrast target through a turbulent environment.

After a wavefront propagates over a turbulent path of length L, its corresponding scintillation index is defined at an arbitrary point of a receiver's entrance pupil as $\sigma_I^2 = \langle I^2\rangle/\langle I\rangle^2 - 1$ (where I denotes the irradiance) [6] and is generally determined in experiments in which the received wavefront is focused on a single-element light detector. Now, we consider the imaging of a high-contrast target through turbulence as a simultaneous acquisition of many independent samples of irradiance by defining a *pixel-based scintillation index*:

$$(\sigma_I^2)_{i,j} = \frac{\langle I_{i,j}^2\rangle}{\langle I_{i,j}\rangle^2} - 1, \tag{1}$$

where $I_{i,j}(t)$ expresses the irradiance over time of an image pixel with coordinates (i, j) given by an optical wave propagating through atmospheric turbulence, and $\langle\cdot\rangle$ is the time average. This definition in imaging terms poses the problem of estimating turbulence intensity with an array of scintillation indices versus the usual single-element method. We find that it is possible to extract C_n^2 information from $(\sigma_I^2)_{i,j}$ after careful selection and counting of its elements as detailed below.

For incoherent imaging though atmospheric turbulence, the intensity of a target image (at the receivers' aperture) will fluctuate the most on high-contrast borders [7] and will barely fluctuate over uniform regions; therefore, the visual representation of $(\sigma_I^2)_{i,j}$ will resemble an edge–filter applied to the target image. To locate and count only the pixels with a relatively high scintillation, a threshold value τ can be applied to this scintillation index representation to define a binary set $\Omega_{i,j} = \{0 \text{ if } (\sigma_I^2)_{i,j} < \tau, \text{ and } 1 \text{ if } \tau \le (\sigma_I^2)_{i,j} < 1\}$ (pixels related to the edges of highest contrast over the imaged target). We shall compare this with the binary output $E_{i,j}$ of a simple edge filter [8] applied to the mean image. It is possible to deduce from [9] that any beam propagating though turbulence has a scintillation index proportional to $C_n^2\, k^{7/6} L^{11/6}$ for the OK model and weak fluctuation regime ($\sigma_I^2 < 1$). Experimental evidence presented in this Letter suggests that the number of thresholded pixels is proportional to this result, according to

$$\gamma(\lambda, L) \cdot \left(\frac{\sum_{i,j}\Omega_{i,j}}{\sum_{i,j}E_{i,j}}\right) = C_n^2\left(\frac{2\pi}{\lambda}\right)^{7/6} L^{11/6}, \tag{2}$$

where C_n^2 is the index of the refraction structure constant and λ is the wavelength. Finally, $\gamma(\lambda, L)$ is a proportionality factor (with no units) which we propose to characterize in laboratory conditions by analyzing the ratio of the amount of non-zero

pixels in $\Omega_{i,j}$ to the amount of non-zero pixels in $E_{i,j}$. In this Letter, we systematically study this factor and find it to be

$$\gamma(\lambda, L) = G_0 \left(\frac{2\pi}{\lambda}\right)^{7/6} L^{11/6}, \quad (3)$$

where G_0 is a *pixel–scintillation structure factor* ($\mathrm{m}^{-2/3}$) to be determined empirically. Knowledge of this factor allows us to estimate C_n^2 simply from Eqs. (2) and (3), according to

$$C_n^2 = G_0 \cdot \left(\frac{\sum_{i,j}\Omega_{i,j}}{\sum_{i,j}E_{i,j}}\right). \quad (4)$$

It is interesting to note that imaging a given fixed target, the factor $\sum_{i,j}E_{i,j}$ as it is defined will provide approximately the same result in a wide range of turbulence conditions, while $\sum_{i,j}\Omega_{i,j}$ may go from 0 to a considerable fraction of the total number of pixels in the image depending on turbulence intensity.

A conceptually simple experiment of laboratory imaging was performed in controlled conditions in which a checkerboard pattern [Fig. 2(a)] is displayed on a standard LCD monitor followed by a region with an artificial turbulence (depicted in Fig. 1) and then focused on an off-the-shelf webcam (Logitech Webcam Pro 9000, 640 × 400 resolution, 30 frames/s).

For the purposes of having fully-developed inertial turbulence at stable and statistically repeatable conditions, we employ a laboratory turbulence chamber (turbulator) similar to the one originally proposed by Fuchs *et al.* [10] and later enhanced by Keskin *et al.* [11]. To simulate the atmospheric turbulence, two air fluxes at different temperatures are forced to collide in the chamber producing an isotropic mix between hot and cold air. The heat source is an electric heater controlled by changing the current passing through it, and the cold channel injects

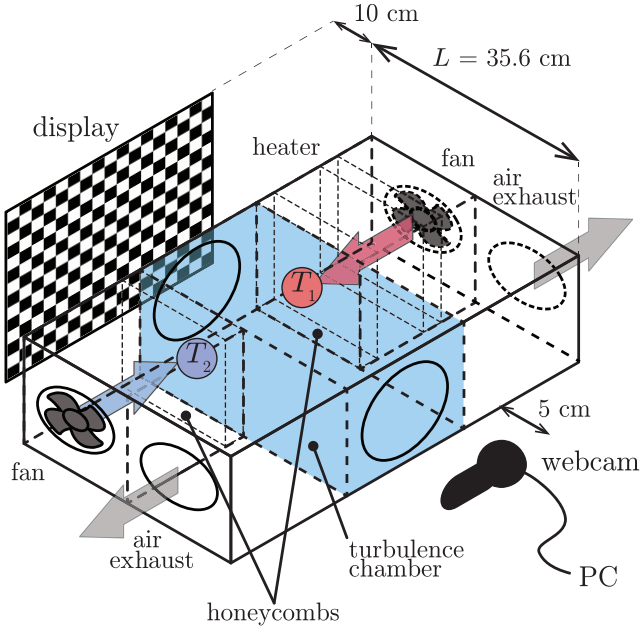

Fig. 1. Experimental setup. The turbulator is suspended from an independent structure in order to avoid any vibration in optics components.

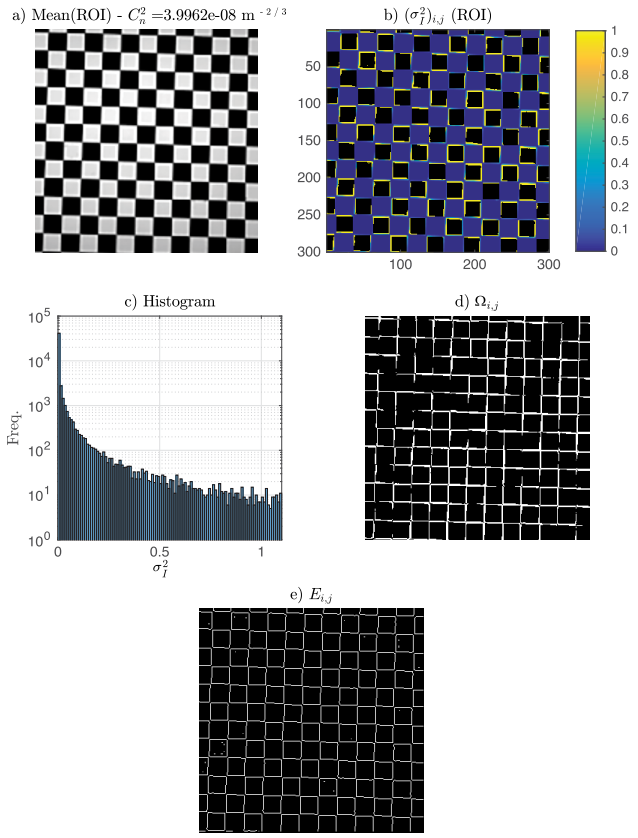

Fig. 2. Representative case of the characterization (out of 13 different settings studied), strongest turbulence condition ($C_n^2 \sim 4 \cdot 10^{-8}$ $\mathrm{m}^{-2/3}$). (a) Average frame of checkerboard in ROI (300 × 300 pixels) affected by turbulence (300 pixels ≡ 15.027 cm). (b) Pixel-based scintillation index image $(\sigma_I^2)_{i,j}$ ($\tau = 0.01$). (Note: a marginal amount of pixels have a value of $(\sigma_I^2)_{i,j} > 1$ and are plotted as 1 for scale clarity.) (c) Histogram of pixel-based scintillation values. (d) Representation of binary mask $\Omega_{i,j}$. (e) Simple edge filter output $E_{i,j}$ applied on mean image (a).

room-temperature air. Light from the target propagates across ∼0.35 m of turbulence in the mixing chamber. Air flow velocity is fixed in this setup because both fans are operated at identical velocities and, therefore, turbulence characteristics are only due to the temperature difference ΔT. By increasing the temperature of the hot source, different turbulence intensities can be achieved. The turbulator offers the advantage of a stable behavior for any C_n^2 value in its operational range, tunable by the user by simply adjusting the temperature parameters, unlike other methods designed to simulate atmospheric turbulence in laboratory conditions [12,13]. The strength of the artificial turbulence, quantified by the refractive index structure constant C_n^2, and the inner and outer scales (l_0 and L_0), were previously estimated following the procedure suggested by Masciadri and Vernin [14] ($l_0 \sim 3$ mm and $L_0 \sim 15$ cm). For such a purpose, a collimated laser beam is propagated through the turbulent layer and then filtered by a variable pupil; the variance of angle-of-arrival fluctuations of the filtered beam is calculated as a function of pupil radii (see Fig. 1 in [14]). By analyzing the averaging effect of the pupil sizes and considering the effects of the inner and outer scales through the von Kármán spectrum, it is possible to estimate the different turbulence

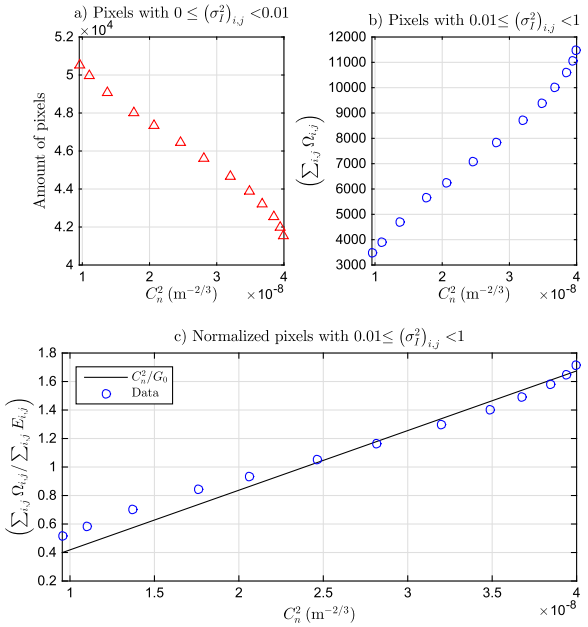

Fig. 3. Amount of thresholded pixels in ROI. (a) Lowest scintillation pixels. (b) Higher scintillation pixels. (c) Normalized higher scintillation pixels with linear fit. The pixel–scintillation structure factor is found to be $G_0 = (2.39 \pm 0.08) \cdot 10^{-8}$ m$^{-2/3}$ ($R^2 = 0.9634$).

parameters (C_n^2, l_0 and L_0) by the fit of the theoretical model (Eq. (12) in [14]) to the empirical variances. Particularly, C_n^2 is expressed as a function of the temperature difference between hot and cold sources ($\Delta T = T_1 - T_2$). Experiments were carried out with 13 temperature differences ranging from 15.5°C to 152.7°C, all with characterized C_n^2 ranging from $9.54 \cdot 10^{-9}$ to $3.99 \cdot 10^{-8}$ m$^{-2/3}$ and calculated σ_R^2(632 nm) ranging from 0.24 to 1.02 (weak to strong fluctuation range). Reference measurements with the fans on and off were captured as well and can be considered as background measurements to quantify the electronic, mechanical noise and room turbulence effects.

To test this technique in an independent case where C_n^2 was not known beforehand, we used a standard electric heater between an LED monitor with the same checkerboard pattern and webcam employed in the characterization, recording at 30 frames/s with a frame of 640 × 400 pixels. The target was at distance $L \sim 0.6$ m and the convective heater operated at full power (2000 W).

In the first case (laboratory imaging), we determined a region of interest (ROI) of 300 × 300 pixels while, in the second case, the ROI was 200 × 200 (due to arrangement constraints). In both cases, we selected the green channel from the RGB output of the camera ($\lambda \sim 510$ nm) for analysis purposes. Averages were taken for 1100 consecutive frames (~36.7 s) [see Fig. 2(a)]. To find $E_{,i,j}$, in all cases we use Matlab's "log" edge filter with default settings; we have tried others, and this one provides the cleanest results in terms of edge detection.

In the case of laboratory imaging, we calculated for each C_n^2 the scintillation index image $(\sigma_I^2)_{i,j}$ [Fig. 2(b)], from which a histogram can be visualized [Fig. 2(c)]. We have carefully studied the histograms and determined that a threshold value $\tau = 0.01$ obtains a binary mask $\Omega_{i,j}$ with enough elements for the analysis [Fig. 2(d)]. We also got the edge filter output from the mean image [Fig. 2(e)]. As expected, we find that the number of pixels with $(\sigma_I^2)_{i,j} < \tau$ decreases with C_n^2 [Fig. 3(a)], while it increases with good linear agreement for pixels with $\tau \le (\sigma_I^2)_{i,j} < 1$ [Fig. 3(b)]. By means of the linear fit of $\sum_{i,j}\Omega_{i,j} / \sum_{i,j}E_{i,j}$ versus C_n^2, we find the pixel–scintillation structure factor Eq. (3) to be $G_0 = (2.39 \pm 0.08) \cdot 10^{-8}$ m$^{-2/3}$ and, therefore, in this condition we get $\gamma(\lambda, L) = 0.64 \pm 0.02$.

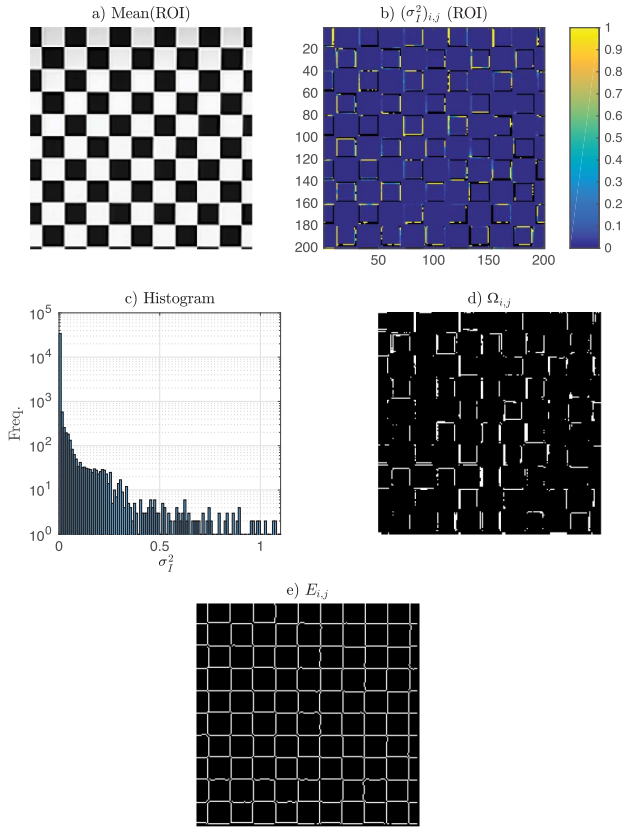

Fig. 4. Independent case. (a) Average frame of checkerboard in ROI (200 × 200 pixels) affected by turbulence (200 pixels ≡ 18.933 cm). Pixel-based scintillation index image $(\sigma_I^2)_{i,j}$ ($\tau = 0.01$). (b) Scintillaton index image $(\sigma_I^2)_{i,j}$. (Note: a marginal amount of pixels have a value of $(\sigma_I^2)_{i,j} > 1$ and are plotted as 1 for scale clarity.) (c) Histogram of pixel-based scintillation values. (d) Representation of binary mask $\Omega_{i,j}$. (e) Simple edge filter output $E_{i,j}$ applied on mean image (a).

In the independent case, we repeat the same analysis described in the previous paragraph [Figs. 4(a)–4(c)] and estimate C_n^2 based on the laboratory estimation of G_0. After examination of the histogram [Fig. 4(c)], we confirm $\tau = 0.01$ as a good threshold value for this case as well. With this method, the structure constant for the index of refraction is found to be $C_n^2 = (1.46 \pm 0.05) \cdot 10^{-8}$ m$^{-2/3}$. This value is in accordance

Table 1. Summary of Results

	Estimated Value
G_0	$(2.39 \pm 0.08) \cdot 10^{-8}$ m$^{-2/3}$
$\gamma(\lambda, L)$	0.64 ± 0.02
C_n^2 (independent case)	$(1.46 \pm 0.05) \cdot 10^{-8}$ m$^{-2/3}$

with an independent estimation based on laser beam wandering variance using the same heater (this method to estimate turbulence strength is described in [15]).

Results are outlined in Table 1.

Summarizing, we have found that the proposed model provides the possibility to use an inexpensive setup to bring a reasonable estimation of C_n^2 taking advantage of the propagation of light from a high-contrast image. We proposed a pixel–scintillation structure factor (G_0) and found its value from experimental data. The ratio $\sum_{i,j}\Omega_{i,j}/\sum_{i,j}E_{i,j}$ in Eq. (4) allows us to estimate structure constants in independent conditions within the linear empirical relationship [Fig. 3(c)]. A next-generation version of the turbulator is currently underway and, in future works, we shall investigate the validity range of this model in lower turbulence conditions.

Funding. Consejo Nacional de Investigaciones Científicas y Técnicas (CONICET), Argentina; Universidad Nacional de La Plata (UNLP), Argentina; Comisión Nacional de Investigación Científica y Tecnológica (CONICYT), Chile (1140917, FONDECYT); Pontificia Universidad Católica de Valparaíso, Chile (123.731/2014); MINCYT-CONICYT Proyecto Bilateral Argentina-Chile (CH/13/05).

REFERENCES

1. G. Galilei, *Sidereus Nuncius, or The Sidereal Messenger* (University of Chicago, 1989).
2. R. Mahon, C. I. Moore, M. S. Ferraro, W. S. Rabinovich, and M. R. Suite, Proc. SPIE **8162**, 81620A (2011).
3. C. N. Reinhardt, D. Wayne, K. McBryde, and G. Cauble, Proc. SPIE **8874**, 88740F (2013).
4. K. McBryde and K. Gibson, Proc. SPIE **8874**, 88740P (2013).
5. K. B. Gibson and S. M. Hammel, Proc. SPIE **9224**, 92240V (2014).
6. L. C. Andrews, R. L. Phillips, and C. Y. Hopen, *Laser Beam Scintillation with Applications* (SPIE, 2001), Vol. **PM99**.
7. M. Charnotskii, Opt. Eng. **52**, 046001 (2013).
8. J. R. Parker, *Algorithms for Image Processing and Computer Vision*, 2nd ed. (Wiley, 2011).
9. M. I. Charnotskii, J. Opt. Soc. Am. A **13**, 1094 (1996).
10. A. Fuchs, J. Vernin, and M. Tallon, Appl. Opt. **35**, 1751 (1996).
11. O. Keskin, L. Jolissaint, and C. Bradley, Appl. Opt. **45**, 4888 (2006).
12. J. Anguita and J. Cisternas, Opt. Lett. **36**, 1725 (2011).
13. R. Barille and P. LaPenna, Appl. Opt. **45**, 3331 (2006).
14. E. Masciadri and J. Vernin, Appl. Opt. **36**, 1320 (1997).
15. G. Funes, M. Vial, and J. Anguita, Opt. Express **23**, 23133 (2015).